Perfusive Electroosmotic Transport in Packed Capillary Electrochromatography: Mechanism and Utility

Daming Li, Vincent T. Remcho
Department of Chemistry, West Virginia University, Morgantown, WV 26506-6045

Received 24 November 1994; accepted 23 December 1996

Abstract: In this study, silica-based packing materials with pore sizes (herein referred to primarily as *channel diameters*, d_{ch}) ranging from 60 to 4000 Å were utilized to elucidate the role of pore size in CEC. Separations were conducted using a commercially available CE system, the inlet and outlet buffer reservoir compartments having been modified to allow constant application of ~150 psi of helium head pressure. This application of pressure was sufficient to prevent nucleation of gas bubbles, a common practical hindrance in CEC. On-column UV detection was performed following the outlet frit of the packed section of the capillary. Electrokinetic sample introduction was employed. The experimental results of these studies indicate that the use of wide-pore media in CEC may provide for notable increases in efficiency. When wide-channel, corpuscular silica packing materials are employed in CEC, the microbeads which comprise the larger particle begin to dictate the "true" or effective diameter of the packing particles, and analytes experience two distinct regions of pore space through which eluent flows: the intraparticle region (inside the particles of packing material) and the interparticle region (between adjacent particles of packing material). The percent of total pore volume contributed by through-pores is likely to be relatively small in the packing materials used, suggesting that particles with a greater degree of perfusive character could provide even further increases in both efficiency and loading capacity. These larger diameter packing materials are easier to work with, less expensive, and offer increased probability of success in the manufacture of packed capillaries for CEC. *J Micro Sep* **9:** 389–397, 1997

Key words: *capillary electrochromatography (CEC); perfusion; bulk transport; porous silica*

INTRODUCTION

Relative to other electrokinetic separation techniques, capillary electrokinetic chromatography [1–5] [CEC, or electroosmotically driven packed capillary high-performance liquid chromatography (HPLC)] has remained largely unexplored. In spite of this, CEC remains a viable technique which is capable of providing efficiencies approaching those typical of capillary electrophoresis, but with the added advantages of separating neutrals and the broad range of retention mechanisms and selectivity typical of HPLC [6–9].

Regardless of the mode of bulk transport employed in liquid chromotographic separations—pressure drive or electrokinetic drive—rate theory predicts that improvements in efficiency may be achieved by utilizing the smallest practically available packing materials. The recent introduction of submicrometer diameter particulates for LC column manufacture has made possible the achievement of unprecedented efficiency in pressure-driven LC separations. Use of these materials in CEC has resulted in even further increases in efficiency as a result of decreased flow velocity inhomogeneity induced zone dispersion. From the practical perspective, however, these submicrometer materials are less than ideal. They have demonstrated a tendency to aggregate and occlude the entrance of capillary column blanks in the process of packing, thus limiting the success

Correspondence to: V. T. Remcho.
Contract grant sponsors: Society for Analytical Chemists of Pittsburgh, U.S. Department of Energy; contract grant number, DE-FC21-92MC29467.

CCC 1040-7685/97/050389-09

rate in production of these columns. As smaller and smaller particle sizes become available, these practical problems will continue to mount.

An alternative to using materials of these small dimensions which is capable of yielding similar results in terms of efficiency enhancement is the employment of wide-pore, large (5–10-μm) particle size packing materials, produced via a variation of the sol-gel method, under conditions which permit perfusive (through-particle) transport of eluent. Elimination of the high pressure drop associated with HPLC makes CEC a gentle technique and makes possible the use of these highly porous media, which are susceptible to crushing in high-pressure applications. The potential benefit of wide-pore packing materials in CEC lies in the elimination of electrochemical double-layer overlap [10] within the pores (Figure 1). This overlap distorts the within-pore flow profile in through-pores to a Poiseuille-like distribution of flow velocities. In the extreme, electroosmotic flow is virtually eliminated. If the pores are sufficiently large and if an appreciable portion of them are through-pores, electroosmotic flow both through and between particles is possible. This perfusive electroosmotic transport serves to minimize plate height by eliminating stagnant mobile phase pools into which analyte molecules may diffuse. This in turn reduces the contribution of slow mass transport to plate height [11].

The microbeads which comprise the larger particle then begin to dictate the "true" or effective diameter of the packing particles, and analytes experience two distinct regions of pore space through which eluent flows: the intraparticle region (inside the particles of packing material) and the interparticle region (between adjacent particles of packing material). These larger diameter packing materials are easier to work with, less expensive, and offer increased probability of success in the manufacture of packed capillaries for CEC.

The experimental results of these studies indicate that the use of wide-pore media in CEC may provide for notable increases in efficiency, as indicated in Figure 2. The percent of total pore volume contributed by through-pores is likely to be relatively small in the packing materials used, suggesting that particles with a greater degree of perfusive character could provide even more impressive increases in both efficiency and loading capacity.

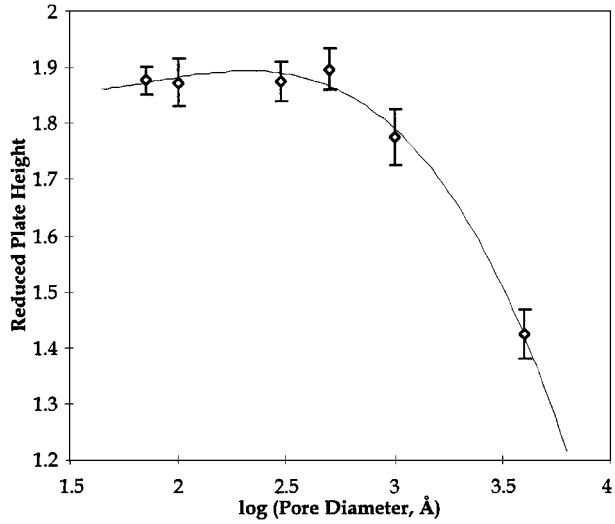

Figure 2. *Effect of increasing pore diameter on plate height in CEC. Data points represent the mean of 10 measurements of h for acetone, an unretained test probe. Error bars indicate standard deviation. Columns employed were packed with 7-μm spherical, porous, C-18 derivatized silica particles and had inner diameters of 75 μm. An 80% CH_3CN/20% 100 mM phosphate buffer (pH 6.9) mobile phase was used. Electroosmotic flow was induced at a field strength of 300 V/cm.*

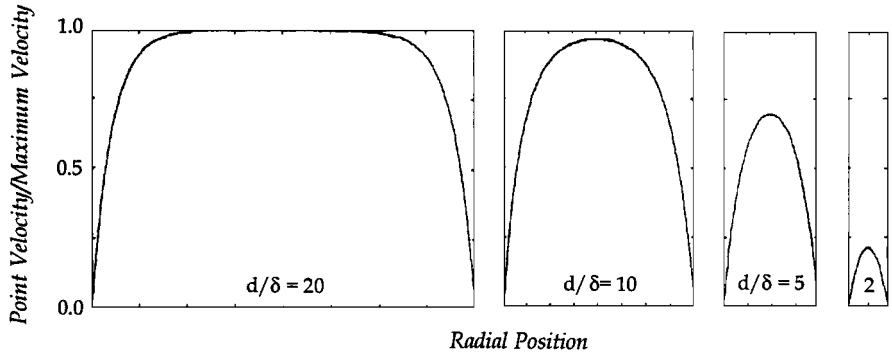

Figure 1. *Effect of electrochemical double-layer overlap on electroosmotic flow velocity as a function of distance from the wall of a liquid-filled pore (d-pore diameter, δ = double-layer thickness) (After ref. 10)*

EXPERIMENTAL

Apparatus. The apparatus used consisted of an in-house modified version of an ATI-Unicam (now Thermo CE, Franklin, MA) Crystal 310 CE system. The inlet and outlet vial assemblies were adapted to allow the application of ca. 150 psi of helium head pressure to the vials. This was accomplished at the inlet by machining a replacment for the standard spring-loaded vial seal from a block of polycarbonate. The block was milled to allow for passage of a platinum wire electrode, a gas inlet line, and the separation conduit and made use of the base of the standard vial seal assembly. A schematic of the adapter is shown in Figure 3. The outlet vial assembly was modified by replacing the standard metal cap with an O-ring-sealed stainless steel fitting with provision for passage of the electrode and capillary and with a compression fitting for attachment of a helium gas line. This adapter is shown in Figure 4. A Linear Instruments (Fremont, CA) model 200 UV detector was used for on-column detection immediately following the outlet frit. Frits were produced and windows for optical detection were created using an arc fusion splicer designed for joining optical fibers (AlcoaFujikura, Tokyo, Japan). Data were collected using a Rainin (Woburn, MA) Dynamax Mac-Integrator II hardware/software package in conjunction with an Apple (Cotati, CA) Power Macintosh 6100/66 computer.

Reagents. Fused silica capillaries (75 μm i.d.) were purchased from Polymicro Technologies (Phoenix, AZ). Nucleosil 4000-7 packing material (Macherey-Nagel, Düren, Germany) was used in the manufacture of end frits, as were Kasil no. 1 water glass (The PQ Corporation, Valley Forge, PA) and formamide (Aldrich Chemical Company, Milwaukee,

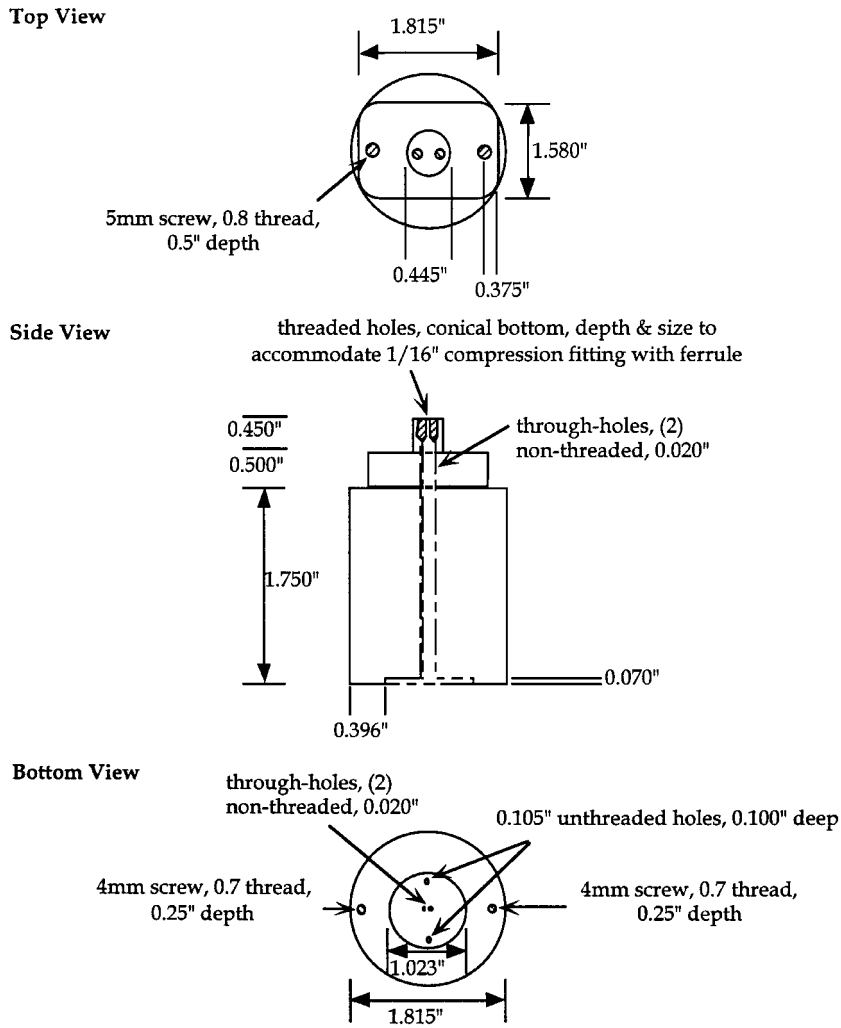

Figure 3. *Schematic showing the structure and dimensions of the high-pressure inlet adapter used in these experiments.*

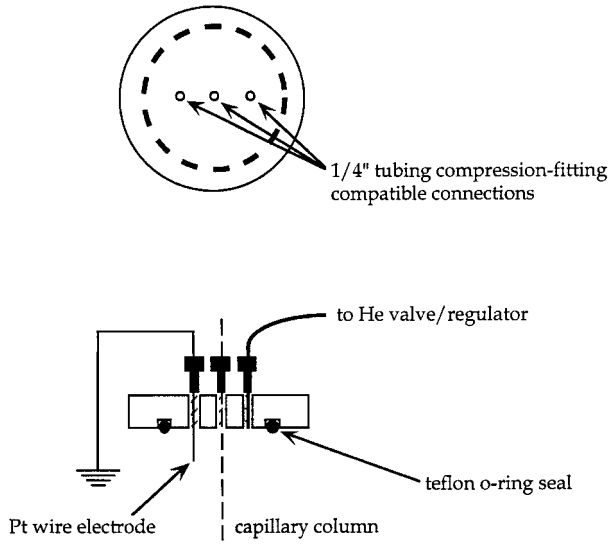

Figure 4. *Schematic showing the structure and dimensions of the high-pressure outlet adapter used in these experiments.*

WI). Nucleosil C_{18} packing materials with pore sizes ranging from 100 to 4000 Å (particle size 3 and 7 μm) were used in most of the columns produced. Also used was a 70-Å-pore-size, 7-μm particle diameter DuPont (Wilmington, DE, USA) Zorbax ODS packing material. The HPLC grade acetonitrile and all buffer preparation reagents were bought from Fisher Chemicals (Fair Lawn, NJ). Buffers were prepared from stock solutions (0.5 M) of monobasic, dibasic, and tribasic sodium phosphates, using the Henderson–Hasselbach equation to determine the appropriate relative amounts of the two necessary stock solutions. Acetone, methyl *p*-hydroxy benzoate, ethyl *p*-hydroxy benzoate, *n*-propyl *p*-hydroxy benzoate, and *n*-butyl *p*-hydroxy benzoate were from Sigma Chemical Co. (St. Louis, MO).

Column manufacture. Fused silica capillaries with inner diameters of 75 μm were cut to a length of 40 cm. Frits were installed at one end of the column as follows:

- 0.01 g Nucleosil 4000-7 silica packing material was mixed with 100 μL water glass and 10 μL formamide, producing a homogeneous mixture;
- the capillary was tapped end downward into the mixture, thus forcing some of the paste into the end of the capillary;
- when the capillary was filled to about 1 mm, the mixture was sintered into place by aligning the nonsintered frit with the electrodes of an arc fusion splicer and heating the mixture for 1 s; and
- after sintering, the capillary was baked in an oven for 2 h at 120°C.

The columns were slurry packed using a procedure similar to that described by Borra and others [12] for preparing capillary columns of larger inner diameter (100–300 μm). A slurry was prepared in a ratio of 80:1 (milliliters to grams) slurry liquid/packing material. Packing materials were slurried in aetonitrile, ultrasonicated for 15 min and transferred to a home-made 10 mm i.d. $\times$ 10 mm long cylindrical reservoir to which the fritted column blank was coupled. The reservoir was then connected to a high-pressure syringe pump (ISCO, Lincoln, NE) which was operated in the constant pressure mode at 3500 psi. The reservoir was placed in an ultrasonic bath to minimize settling out of the slurry while packing took place. The particles going into the column were observed with a zoom stereomicroscope periodically throughout the packing process to ensure that no voids has formed. Once the desired length of the column was filled, the pressure was maintained for 30 min in order to consolidate the packed bed, and an outlet frit was made using the fiber-optic fusion splicer to sinter a portion of the packing material. Following this, the pump was turned off and the pressure allowed to slowly decrease for another 30 min. The column was then removed from the packing apparatus and flushed with mobile phase (20:80 CH_3CN:100 mM sodium phosphate buffer, pH 6.9) at 3500 psi, and a narrow (0.5-mm) detection window was made immediately adjacent to the outlet frit, again using the fusion splicer.

RESULTS AND DISCUSSION

That perfusive flow is possible in wide-pore silica packing materials is a direct consequence of the method in which many of these materials are manufactured. In many instances, spherical silica packing materials for use in chromatography are manufactured by [13–17]

1. polycondensation and polymerization of silicic acids to form a silica sol comprised of discrete, nonporous, amorphous silica beads; followed by
2. controlled aggregation of colloidal silica to form a hydrogel consisting of spherical multiplets of nonporous silica beads (particles); and
3. washing and drying of the aggregated particles to yield hard, porous spheres.

This in turn may be followed by various surface modification chemistries for the production of packing materials tailored for specific tasks. Regardless of the type of bonded phase eventually applied, the gross structure of the packing material remains corpuscular in nature [18], being comprised of a regular arrangement of tightly packed spheres which define

the pore space (Figure 5). The critical factors determining pore size and geometry then become the size of the original colloidal silica used in making the particles and the number of contact points between adjacent beads in the larger particle (the coordination number). The coordination number in turn defines the porosity of the packing material, which for most column packings is accepted to be $\varepsilon_{tot} = 0.8$ [19], corresponding to largely plane triangular and tetrahedral arrangements of beads (Table I). This pore space is not entirely unlike (though it is much smaller than) the interstitial pore space between packing particles in the packed bed. It stands to reason then that electroosmosis may be supported in this pore space as it is in the interstitial space if only the pores are large enough to preclude overlap of the eletrochemical double layer [10]. Advantages of perfusive transport which make it appealing are (1) the possibility of increased efficiency due to dramatically reduced "effective" particle diameter (arising from the small beads comprising each particle); (2) the greater ease of packing large-particle-size materials (5–10 μm d_p) relative to very small ones (< 2 μm d_p), which should lead to increased success in manufacturing these types of columns; and (3) a possible increase in sample-loading capacity as a result of increased analyte transport into the pore space, leading to an increase in effective accessible surface area. In order to explore the phenomenon of perfusive electroosmosis, a range of materials alike in all aspects other than pore size (to the extent that this is possible) was employed. For purpose of reference, a set of three packing materials of like pore size but differing in particle diameter was also studied. An accounting of all of the columns prepared for the study is provided in Table II.

Dependence of linear electroosmotic flow velocity on field strength. Columns packed with 3 μm (d_p)/100 Å (d_{ch}) Nucleosil C_{18}, 5 μm/100 Å Nucle-

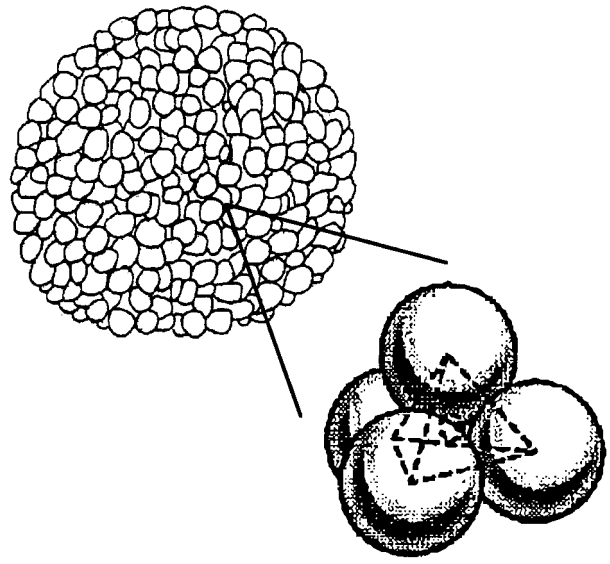

Figure 5. *Diagram of a single spherical, corpuscular particle of packing material, with an expanded view showing one possible geometric arrangement of individual beads comprising the particle. The small circle at the center of the tetrahedron denotes the interparticle channel space.*

Table I. *Several possible geometric arrangements of closely packed spheres and corresponding coordination numbers and porosities.*

Coordination no. (n)	Packing geometry	Porosity of medium (ε_p)[a]
8	face centered cubic	0.320
6	simple cubic	0.475
4	tetrahedral	0.660
3	trigonal planar	0.815

[a]Calculated from $\varepsilon_p = V_p/(V_p + V_s)$, where ε_p is the particle porosity, V_p the specific pore volume, and V_s the volume of the pure solid per gram.

Table II. *Packed capillary columns prepared for use in studying perfusive electroosmotic transport.*

Packing material	Particle size, d_p (μm)	Channel size, d_{ch} (Å)	L_{bed} (mm)	L_{det} (mm)	L_{tot} (mm)
Nucleosil[a]	3	100	196	201	300
Nucleosil[a]	5	100	251	254	310
Nucleosil[a]	7	100	233	235	300
Zorbax[b]	7	70	258	261	315
Nucleosil[a]	7	100	233	235	300
Nucleosil[a]	7	300	227	228	300
Nucleosil[a]	7	500	241	243	310
Nucleosil[a]	7	1000	210	212	300
Nucleosil[a]	7	4000	272	274	310

[a]Nucleosil C18, Macherey-Nagel.
[b]Zorbax ODS, DuPont.

osil C_{18}, and 7 μm/100 Å Nucleosil C_{18} were each operated under identical sets of conditions in order to determine the relationship between field strength and linear velocity of electroosmosis. Field strengths ranging from 150 to 500 V/cm were employed. Acetone was employed as an unretained neutral (zero net electrophoretic mobility) marker; the test mixture also contained methyl paraben and ethyl paraben. A mobile phase consisting of 20% CH_3CN/80% 100 mM phosphate buffer, pH 6.9, was used throughout. No attempt was made to thermostat the capillary.

Not surprisingly, it was noted that a linear relationship existed between field strength and linear velocity over the range of field strengths studied (Figure 6). More importantly, it was also determined that packing material particle size had no effect on linear velocity for the range of particle diameters studied. This led to the conclusion that the interstitial pore space, between adjacent particles of packing material, was sufficiently large to promote electroosmosis.

Effect of packing material particle diameter on plate height. The columns used in determining the dependence of flow velocity on field strength were also employed in studying the effect of particle diameter on plate height in CEC. As expected, the well-established tenets of rate theory hold true for

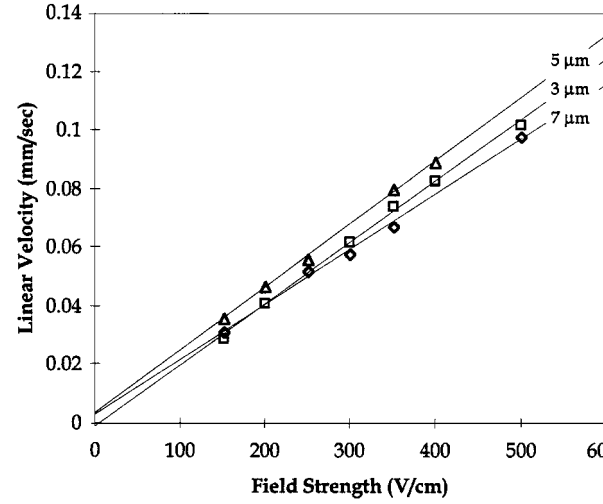

Figure 6. *Linear velocity as a function of field strength for 3-, 5-, and 7-µm-diameter Nucleosil C18 particles.*

CEC as they do in conventional HPLC: Smaller particle sizes yield lower minimum plate heights (Figure 7). The very shallow slope of the mass transfer dominated portion (high-velocity region) of the rate curves is notable in CEC and arises because of a radical decrease in flow velocity inhomogeneity near the surface of the packing particles relative to that at the center of the interstices.

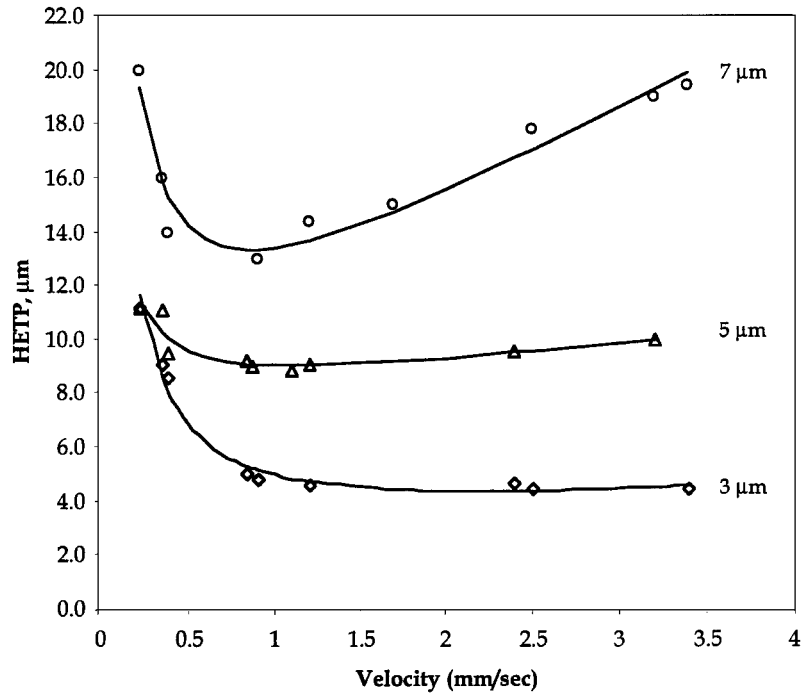

Figure 7. *Plate height as a function of linear velocity for three particle sizes (3, 5, and 7 µm) of Nucleosil C18. In CEC, as in all chromatographic separation methods, smaller particle sizes yield increased efficiency.*

Efficiency enhancements arising from perfusive transport. Columns packed with 7 μm (d_p)/100 Å (d_{ch}) Nucleosil C_{18}, 7 μm/300 Å Nucleosil C_{18}, 7 μm/500 Å Nucleosil C_{18}, 7 μm/1000 Å Nucleosil C_{18}, and 7 μm/4000 Å Nucleosil C_{18} were each operated under identical sets of conditions in order to study perfusive electroosmotic transport. Field strengths in the range of 100–500 V/cm were needed to generate the range of velocities desired. The elution time and peak width for the neutral electroosmotic flow (EOF) marker were used in all calculations to yield the data displayed in Figure 8, a plot of plate height as a function of linear velocity.

As all of the columns generated for use in construction of this plot were packed with 7 μm (d_p) Nucleosil C_{18} packing materials, it might be expected that nearly coincident rate equation curves would result. In the event, however, that perfusive transport of analyte and eluent were occurring, a decrease in eddy diffusion-induced and slow mass transfer-induced zone spreading would be predicted. Decreases in the contributions of each of these two terms to total plate height would be manifest in the high-velocity side of the rate curve, resulting in a decreased slope in this region and a lower minimum in the H-vs.-μ plot. This is in fact what is seen in Figure 8, which supports the argument for perfusive transport in wide-pore (wide-channel) media. In effect, the silica beads comprising the larger particle of packing material are acting as the "true" packing material, decreasing the effective particle size of the packing and improving performance in accord with rate theory. The effect is maximized in the 4000-Å-channel-diameter media, where many of the accessible channels are large enough to preclude excessive electrochemical double-layer overlap and support electroosmosis. In the narrower pore size materials, a much smaller fraction of the pores are wide enough to prevent double-layer overlap, and a decrease in achievable efficiency results. Essentially no benefit is seen when 500-Å-pore-size media are compared to 100- and 300-Å media, as would be expected if there were no perfusive flow.

The most direct means of displaying the positive effect of perfusive transport is to plot the reduced plate height for the series of columns prepared as a function of log(channel diameter). A plot of this type (all columns being operated under identical

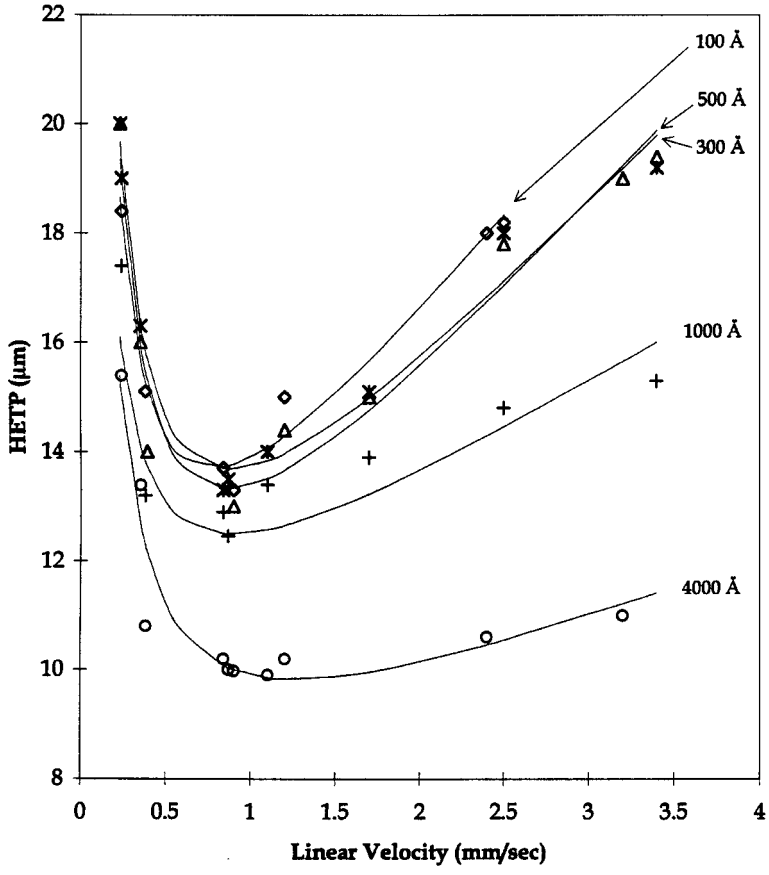

Figure 8. *Plate height as a function of linear velocity for five different pore (channel) sizes of 7-µm-particle-size Nucleosil C18.*

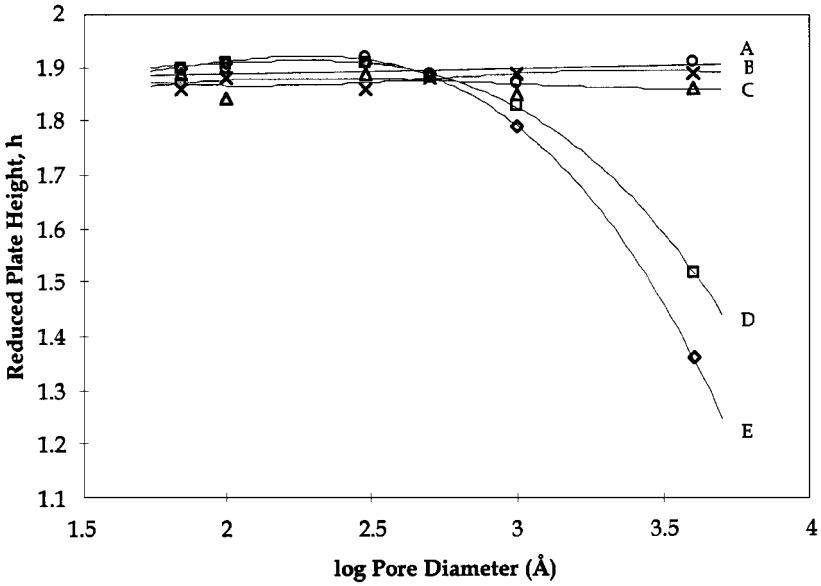

Figure 9. *Reduced plate height versus log (pore diameter) for various buffer concentrations: A, 10 mM; B, 50 mM; C, 100mM; D, 300mM; E, 500 mM. At low buffer ionic strength, where the double layer is thicker, perfusive transport is diminished. This results in a loss of efficiency.*

conditions of mobile phase composition, field strength, and temperature) is shown in Figure 2. This figure clearly illustrates the performance benefit of perfusive electroosmotic transport: a significant improvement in efficiency.

Effect of buffer ionic strength on plate height. The thickness of the electrochemical double layer obviously plays a significant role in perfusive transport through narrow channels. In an effort to verify the origin of the efficiency enhancements noted above as arising from perfusion, a study was conducted in which the ionic strength of the buffer component of the mobile phase was varied over a relatively wide range (10–500 mM). At low ionic strengths, where the double layer is at its thickest, it was expected that some of the perfusive character of a packing material sitting on the cusp of completely supporting perfusive behavior would be lost to excessive double-layer overlap. Under the opposite condition —at high buffer ionic strength—it would then be expected that this same packing material would yield greater perfusive character and therefore provide smaller plate heights. Figure 9 depicts the relationship between reduced plate height (HETP/d_p) and channel diameter (d_{ch}) for phosphate buffers of various concentrations between 10 and 500 mM. For the materials with pore sizes sufficiently large to support electroosmosis, buffer ionic strength (and therefore double-layer thickness) exerted a pronounced effect on efficiency. This would only be predicted for a situation in which perfusion contributes to bulk transport, since the interstitial pore spaces (those between adjacent particles of packing material) would, for all of the buffer ionic strengths employed, be sufficiently large to support unencumbered electroosmosis.

It seems well founded that perfusive electroosmotic transport is occurring in the wide-pore media studied and that it leads to a notable enhancement of efficiency.

CONCLUSIONS

Silica-based packing materials having channel diameters (pore sizes) ranging from 60 to 4000 Å were utilized to elucidate the role of pore size in CEC and to demonstrate the feasibility and utility of perfusive electroosmotic transport. It was shown that corpuscular silica packing materials of large channel diameter (> 2000 Å) are capable of supporting perfusive (through-particle) electroosmosis, which in turn results in a significant increase in efficiency. Other advantages inherent to perfusive transport include greater ease of packing large-particle-size materials (5–10 μm d_p) relative to very small ones (< 2 μm d_p) and a possible increase in sample-loading capacity as a result of increased analyte transport into the pore space, leading to an increase in effective accessible surface area.

ACKNOWLEDGMENTS

The authors thank the Society for Analytical Chemists of Pittsburgh (SACP) and the US Depart-

ment of Energy (under contract no. DE-FC21-92MC29467) for financial support of this research.

REFERENCES

1. J.H. Knox and I.H. Grant, *Chromatographia* **24**, 135 (1987).
2. J.H. Knox and I.H. Grant, *Chromatographia* **32**, 32 (1991).
3. M.M. Dittmann and G.P. Rozing, *J. Chromatogr. A* **744**, 63 (1996).
4. N. W. Smith and M. B. Evans, *Chromatographia* **414**, 197 (1995).
5. R.J. Boughtflower, T. Underwood, and J. Maddin, *Chromatographia* **41**, 398 (1995).
6. M.M. Robson, S. Roulin, S.M. Sheriff, M.W. Raynor, K.D. Bartle, A.A. Clifford, P. Myers, M.R. Euerby, and C.M. Johnson, *Chromatographia* **43**, 313 (1996).
7. V.T. Remcho, W.H. Wilson, and H.M. McNair, *J. High Resol. Chromatogr.* **13**, 442 (1990).
8. V.T. Remcho, N.E. Ballou, G.R. Ducatte, and C. Quang, *J. High Resol. Chromatogr.* **19**, 183 (1996).
9. D. Li and V.T. Remcho, *J. Chromatogr. B*, in press.
10. C. Rice and R. Whitehead, *J. Phys. Chem.* **69**, 4017 (1965).
11. J.C. Giddings, *Dynamics of Chromatography*, *Part I*: *Principles and Theory* (Marcel Dekker, New York, 1965).
12. C. Borra, M.H. Soon, and M. Novotny, *J. Chromatogr.* **385**, 75 (1987).
13. R.K. Iler, in *Surface and Colloid Science*, Vol. 6, E. Matijevek, Ed. (Wiley, London, 1973).
14. K. Unger and J. Schick-Kalb, German Patent, No. 2,155,281 (1971).
15. J.J. Kirkland, U.S. Patent, No. 3,782,075 (1974).
16. K. Unger and B. Scharf, *J. Colloid Interface Sci.* **55**, 377 (1976).
17. D. Barry, in *Characterization of Powder Surfaces*, G.D. Parfitt and K. S. W. Sing, Eds. (Academic, London, 1976, p. 350.
18. K.K. Unger, *Porous Silica*: *Its Properties and Use as a Support in Column Liquid Chromatography* (*Elsevier*, *Amsterdam*, 1979).
19. *V.R. Meyer*, *J. Chromatogr.* **332**, 197 (1985).